A Numerical Experiment Study for Effects of the Grassland Desertification on Summer Drought in North China①

Zheng Weizhong (郑维忠)

Department of Atmospheric Sciences, Nanjing University, Nanjing 210093

Ni Yunqi (倪允琪)

Chinese Academy of Meteorological Sciences, Beijing 100081

(Received February 20, 1998; revised June 20, 1998)

ABSTRACT

In this paper, the summer climate of 1991 in North China is simulated by using the high-resolution regional climate model (RegCM2) and the effects of the grassland desertification on summer drought in the central and the northern parts of North China as well as Mongolia are studied. It shows that the regional climate model essentially catches the characteristics on distribution and seasonal variation of the precipitation that keep good agreement with the observation. The desertification makes precipitation in the central part of North China during its flood period decrease obviously in July. The border of the precipitation or the soil moisture reduction in the desertification region extends about one latitude southeastward and beyond the southeast edge of the desertification. Thus, vegetation in the border region approaches desertification further. However, there appears evident difference of variation of precipitation over the whole desertification region. The grassland desertification greatly changes the transfers of fluxes between land and atmosphere. The secondary circulation or secondary circulation cells in the desertification region are excited and as a result moisture transport is changed. The variation of flux transfers between land and atmosphere as well as the vertical motion of atmosphere is closely related to that of precipitation.

Key words: Numerical Experiment, Drought in North China, Grassland Desertification

1. Introduction

Many observations and studies indicate that the summer rainfall in North China decreases significantly during recent twenty years. The obvious reduction tendency can be seen from the variation of percentage of summer rainfall anomaly (June-August) in the plain of North China from 1951 to 1988 (Ye and Chen, 1992). Almost no year there is in which the anomaly is above normal in 1980's and there appears clearly drought evidence. Having studied the average distribution on drought and flood during the period of 1979-1988, Wang Shaowu indicates that disasters of droughts and floods occur mainly in North China and South China, especially in the plain of North China where the frequency of drought occurrence is higher and its persistent period is longer (Wang, 1990).

North China is situated in the middle and lower reaches of the Huanghe River Basin. Its underlying surface is characterized by desert in the western, grassland in the central and the

①This work was supported by the National Key Project "Study on Defence Technique for Agrometeorological Disasters".

northern, and forest in the eastern. The demarcation lines of forest, grassland and desert are very distinct. They are roughly in the direction of the northeast–southwest (Ye, 1992). The climatic disasters in North China are no doubt affected by the large scale global climate changes. It is, however, worthwhile to point out that occurrence frequency of the disasters is progressively becoming high as the ecosystem environment changes incessantly. Particular attention must be paid to the effects of regional changes on underlying surface. The desertification phenomenon has become an important part in global environment change (Ye, 1992). It changes greatly the physical features on the land surface, breaks the energy balance of the surface radiation and induces climate and environment changes whose feedback, however, can further accelerate the desertification progress, just as Charney points out the biophysical feedback mechanism (Charney, 1975). It is seen from the areas threatened with desertification over the world that the severe desertification in the eastern Asia appears in North China and Mongolia where grassland vegetation is seriously degraded, particularly for the semiarid belt of alternation between agriculture and pasture (UNFAO, 1977).

In this paper we first analyse the observed precipitation in North China during recent 17 years (1979–1995) with the method of orthogonal rotated principal components analysis (REOF). Then, the summer climate of 1991 chosen as a case is simulated by using a high-resolution regional climate model (RegCM2). Finally, a sensitivity experiment of effects of desertification on the regional climate in North China is completed after the grassland vegetation in both North China and Mongolia is replaced by desert. Thus, occurrence rule and mechanism of droughts in North China are studied.

2. Characteristic of summer precipitation anomaly in North China during recent 17 years

The data set of the observed precipitation during the period of 1979–1995 is a grided field of global monthly average. It is obtained by merging several kinds of individual information sources including gauge observations, satellite estimates and numerical models outputs (Xie and Arkin, 1997). Its resolution is $2.5° \times 2.5°$. This paper chooses the range of 35°–45°N and 105°–120°E from the data set to express North China within which 5×7 points are included. REOF analysis is carried out after the precipitation field is taken anomaly then standardized.

Figure 1a is the temporal variation of the standard anomaly of precipitation in North China from 1979 to 1995. It shows that from the beginning of 1980 to 1986 the anomaly is essentially below the average. The precipitation obviously decreases, especially in 1985 when the negative anomaly reaches −0.60 or so. After that time the anomaly alternates between positive and negative. The largest positive anomaly appears in 1990 and it is an unusual flood year. The precipitation decreases again after 1990.

In order to understand types of the summer drought distributions in North China, the method of REOF is used to analyze spatial character of precipitation. This kind of method has several advantages over the traditional Empirical Orthogonal Functions (EOF) in revealing local features (Ye, Wang and Li, 1997). Figures 2a–c and 1b–d are first three spatial modes obtained by the REOF analysis and related variability of temporal coefficient, respectively. They indicate that the first spatial pattern is characterized with obvious contrast between the Great Bend of the Huanghe River (Hetao) and other areas of North China. It can

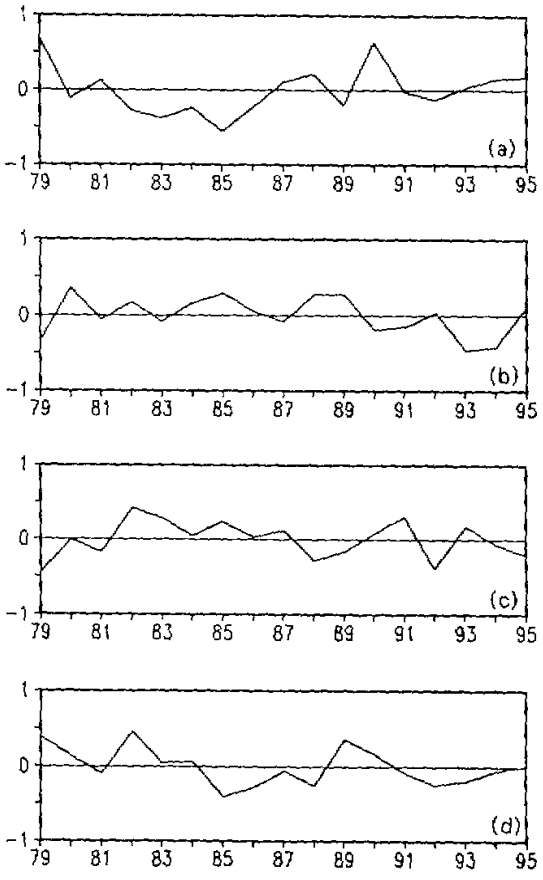

Fig. 1. Temporal variability of summer precipitation in North China during the period of 1979–1995. (a) percentage of precipitation anomaly; (b) the first temporal coefficient; (c) the second temporal coefficient; (d) the third temporal coefficient.

be seen from the temporal variability that the anomaly varies approximately from positive to negative around 1990, as indicates in the most years of 1980's floods appearing in Hetao and droughts in other areas of North China. However, the cases in 1990's are just opposite. The second spatial pattern shows that precipitation anomaly in the southeastern part of North China is contrary to that in the most other parts. Its temporal variability in Fig. 1c indicates that droughts during the period of 1982 to 1986 have this type of acid characteristic. It alternates between drought and flood after 1987. The third spatial pattern reflects that drought and flood pattern in the southern part of North China is opposite to that of the northern part.

The precipitation field reconstructed with first five characteristic modes shows essentially features of summer in 1991. It clearly indicates that rainfall is below normal in the central and the western parts of North China as well as in the middle reaches of Huanghe River. In fact, Mei-yu along the Changjiang-Huaihe River Valley in 1991 began much more earlier than normal years. In June, rainfall was obviously above normal in the Huaihe River, the Hanshui River and the lower reaches of the Changjiang River Valleys. It was clear sky often in the

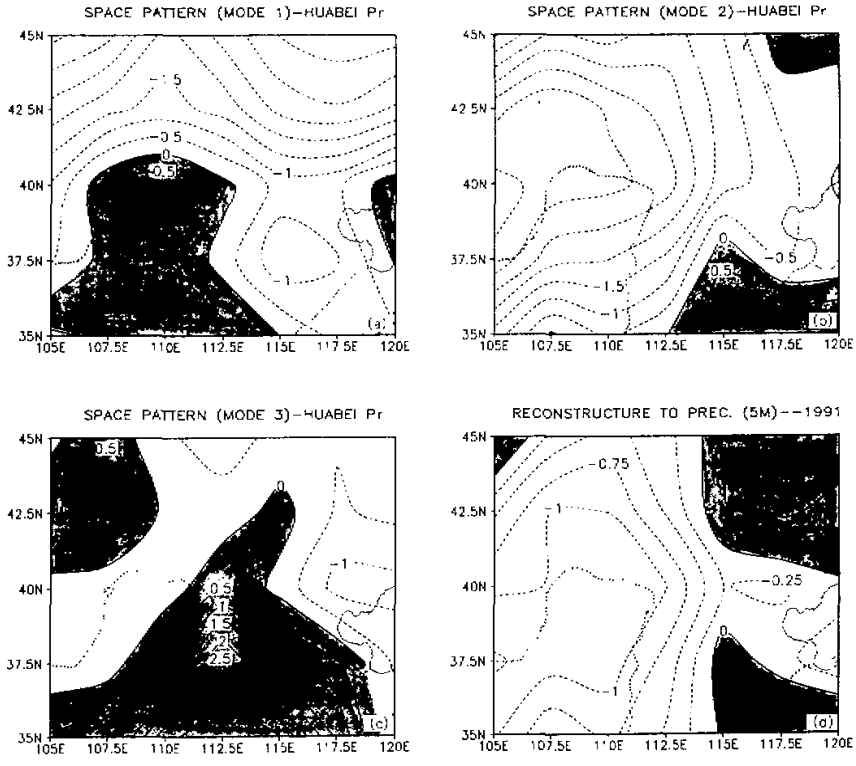

Fig. 2. Spatial character of summer precipitation in North China during the period of 1979–1995.(a) the first spatial pattern; (b) the second spatial pattern; (c) the third spatial pattern; (d) summer precipitation field reconstructed in 1991.

most part of North China. Rainfall was 50% to 100% above normal in the northern part of the North China and 10% to 60% below normal in the southern part. It was also above normal in the western part of Northeast China. In July, rainfall was 30% to 70% below normal in the western part of North China and 40% to 100% above normal in the eastern part. Low temperature and rainy occurred in the most part of Northeast China. In August, rainfall in the most part of China lain to the 100°E east approached or was obviously below normal. Less rainfall appeared in the flood period in the most part of North China, Northeast China and so on. The monthly rainfall was 20% to 90% below normal. Surface air temperatures in North China, Northeast China and so on were above normal. Their monthly average surface air temperatures in the central and the northern parts of North China as well as the plain of Northeast China were 2 to 3°C above normal at the same time.

3. Numerical model and experiment design

The model used in this paper is a second-generation regional climate model (RegCM2) which is developed by Girogi, Marinucci and Bates (1993) at the National Center for Atmosphere Research

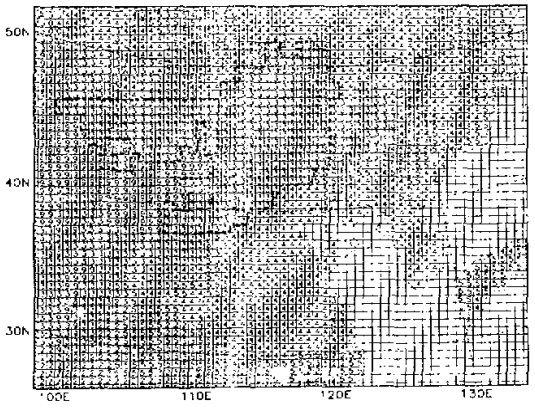

Fig. 3. Model land-use distribution. Land-use types are 3-grassland, 4-deciduous forest, 5-coniferous forest, 9-desert, 0-tundra, and 2-tropical or subtropical forest. The region circled with dash line denotes desertification.

(NCAR). The model uses a σ-coordinate in the vertical direction, $\sigma = (P - Pt) / (Ps - Pt)$, where Ps is the prognostic surface pressure and Pt is the pressure specified to be the model top. Its physical processes include detailed radiative transfer package, the Biosphere-Atmosphere Transfer Scheme (BATS) and so on. The model incorporates the split-explicit time integration technique so that it runs more efficiency. We choose a domain of 3000 km × 3600 km size centered in North China at 41°N and 116°E with a horizontal grid-point spacing of 60 km (Fig. 3). The vertical structure of the model is taken nonuniform with 10 levels. Its full sigma level values are 1.0, 0.99, 0.97, 0.93, 0.85, 0.75, 0.60, 0.45, 0.30, 0.15 and 0.0 with model top at 100 hPa. A Kuo-type cumulus parameterization is used in the RegCM2, along with a simple scheme for resolvable scale precipitation, whereby all water in excess of saturation at a given grid point instantaneously precipitates.

The analysis data of the European Center for Medium-Range Weather Forecasts (ECMWF) are used as initial and lateral boundary conditions necessary to drive the model runs. The driving data having a resolution of 2.5° × 2.5° in the horizontal, are distributed on 7 pressure levels, and are available at intervals of 12 hours. The bilinear technique is employed to interpolate horizontally wind components, geopotential height, temperature and relative humidity to the model grid. Vertical interpolation is linear in pressure for wind and relative humidity, and in the logarithm of pressure for temperature. The model runs from 00 GMT, June 1 to 00 GMT, August 31 of 1991 and the period of simulation is 91 days. Two numerical experiments are carried out. One is a control experiment in which underlying surface is taken as real physical features obtained by interpolation of NCAR land-use distribution with a resolution of 0.5° × 0.5° (see Fig. 3). The other is a sensitivity experiment of grassland desertification. According to distribution of regions threaten by desertification over the world severe degradation of grassland vegetation occurs primarily in North China and Mongolia. Thus, grassland vegetation in the central and the northern parts of North China as well as Mongolia is replaced by desert, that is, land-use type 3 is replaced by 9 within a domain circled with dash line as shown in Fig.3. Impact of grassland desertification can be discussed by comparing sensitivity experiment with control one.

As to land-use types of grassland and desert, both physical features have distinct differences. The

table in the reference (Dickinson, Henderson-Sellers and Kenedy, 1992) gives their physical parameters, where grassland in this paper corresponds to short grass (its type is 2), and desert corresponds to semi-desert (its type is 11) in the reference. One of the most significant changes is increase of surface albedo after the substitution of desert for grassland. Values of surface albedo at the land gird points in the BATS are determined from the albedo of vegetation and the albedo for bare soil in proportion of fractional vegetation cover. Moreover, the albedo for bare soil also depends upon soil type and soil wetness. Considering dry soil and neglecting effect of soil moisture, for example, the visible solar surface albedo ($\mu < 0.7\mu m$) increases from 0.12 for grassland to 0.215 for desert, and the near-infrared surface albedo ($\mu \geq 0.7\mu m$) increases from 0.32 for grassland to 0.43 for desert. The variations of surface albedo no doubt break energy balance between land and atmosphere, thus affecting climate and environment changes.

4. Simulation of impact of grassland desertification on precipitation

As mentioned above we simulate the summer climate of 1991 in North China with real underlying surface for control experiment. Analyses of average monthly precipitation or accumulated summer precipitation simulated by the model all show that the RegCM2 basically catches the features of regional distribution and seasonal variation of precipitation that are essentially in accord with the observation. Figures 4a-b are accumulated summer precipitation simulated and observed respectively, where the filter analysis is used for simulated precipitation. At each of model grid points, the average of 5×5 points is made for outputs of the model. It can be seen from the figures that the model reproduces the regional characteristic on precipitation. An intensive rainband in the direction of the east-west appears in the middle and lower reaches of Changjiang River. Warm-wet air from the southeast can not easily reach the northwestern part of North China due to resistance of Taihang Mountains, so it is an arid region. Another intensive rainband appears along Taihang Mountains. There is less rainfall in Jiaodong peninsula. The rainfall simulated shows that heavy rain from the model is weaker than the observed. Specifically, the Mei-yu rainband along the Changjiang-Huaihe River Valley is obviously weaker than the observed.

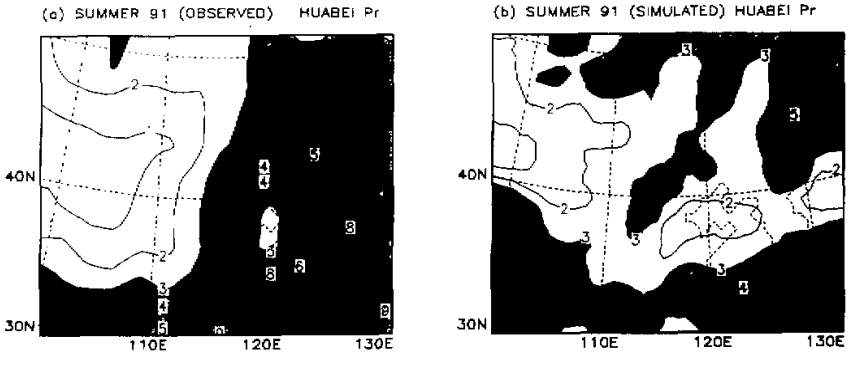

Fig. 4. Summer precipitation in 1991: (a) observation; (b) control experiment. The contour interval is 1.0 mm / day.

Under condition that grassland vegetation in the central and the northern parts of North China as well as Mongolia becomes desertification, the variation of the whole summer precipitation is obvious, especially during the flood period in North China in July, as shown in Fig.4. Rainfall in the southeastern part of the desertification region decreases significantly and a maximum of negative anomaly is more than −1mm / day. Fig. 3 shows that the southeastern edge of the desertification region is located at 40°N and 115°E or so. Therefore, the southeastern border of rainfall reduction area in the desertification region is not coincident with that of the desertification region but extends about one degree southeastward. In similar way, variation of soil moisture in the desertification region also indicates that the border of its reduction extends about one degree to the southeast. From the point of view of desertification process, the decreases of both rainfall and soil moisture do not help plants near the border region to grow and make the vegetation become desertification further. This can, in some degree, explain why the desertification region expands southeastward, that is, a feedback mechanism of desertification. Additionally, the variation of rainfall in the desertification region is nonuniform. Rainfall in the northern part of North China, that is, near 44°N, increases instead and decreases again on the north. Meanwhile, besides North China, it intensifies clearly in the most part of the Changjiang−Huaihe River Valley, the Bohai Gulf and some part of Northeast China.

Along the direction of east−west in the model domain that is roughly in the range from 101°E to 123°E at the center of North China, we average the rainfall and get the variation of rainfall as a function of latitude. Figs. 6a−d show differences between desertification experiment and control one. It is more clearly from the figures that the notable effect of desertification on longitudinal variation of rainfall is in June and July. In June, rainfall increases in the middle and lower reaches of Changjiang River Valley and decreases in the southern part of North China. The intensive rainband during Mei−yu period is inclined to move southward relative to that of control experiment. In July, the average rainfall decreases about 15 mm in the longitudinal range from 38°N to 43°N, that is, the central North China. It demonstrates further that the border of rainfall reduction moves southward about one degree with respect to the southern border of the desertification. Precipitation in the most parts of North China does not change much in August. More obvious variation appears in the northern part

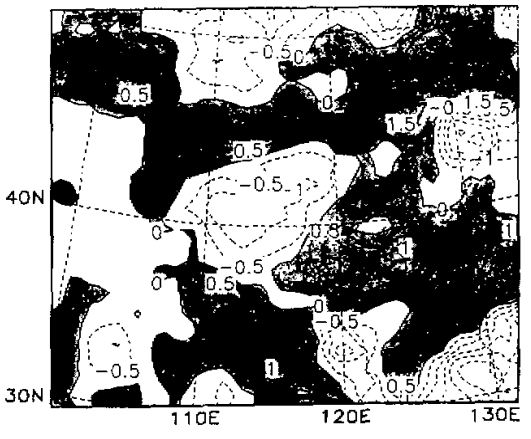

Fig. 5. Difference of precipitation between desertification experiment and control experiment in July. The contour interval is 0.5 mm / day.

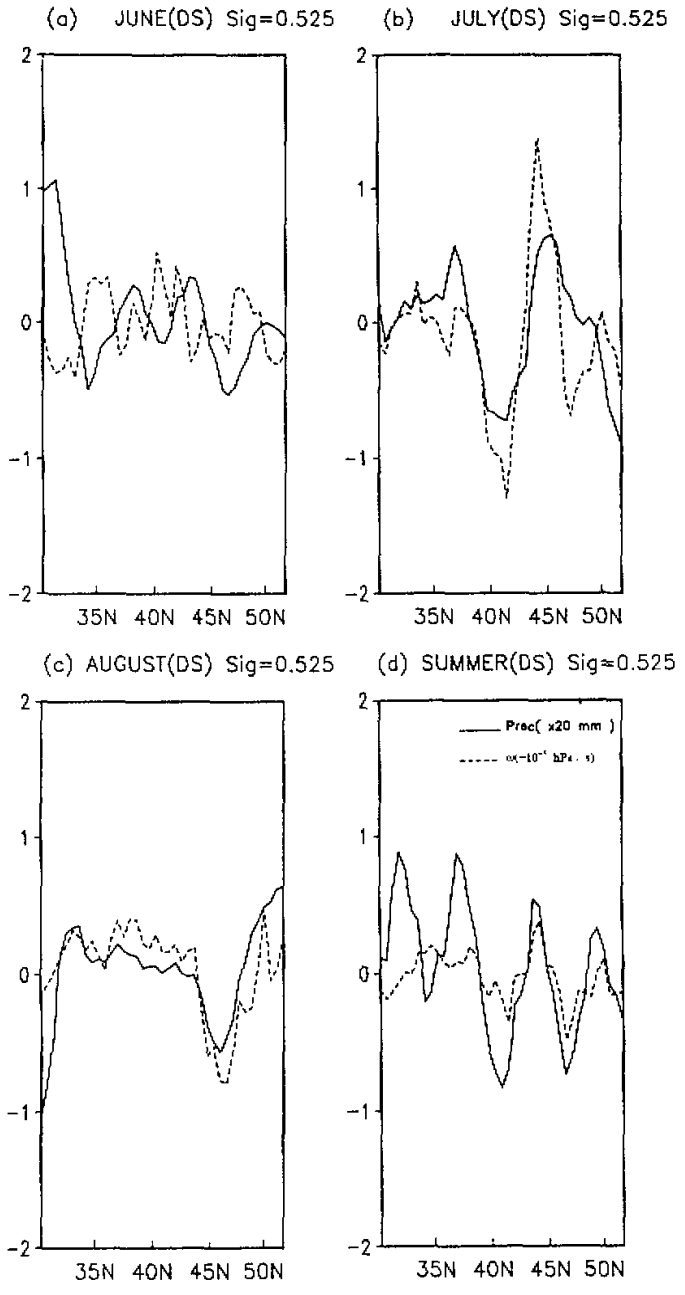

Fig. 6. Anomalies of average rainfall and vertical velocity ω as a function of latitude. (a) June; (b) July; (c) August; (d) summer. The solid line denotes rainfall and the dashed line denotes vertical velocity on $\sigma = 0.525$ model level.

and the average rainfall decreases about 10 mm. Hence it is much complicated for the variation of the whole summer precipitation. The variation of the average rainfall fluctuates as a function of latitude, as shown in Fig.6d.

5. Effect of desertification on transfers of fluxes between land and atmosphere as well as characteristic on variation of atmospheric circulation

As to the experiment of grassland desertification, a direct effect is to increase local surface albedo. Soil moisture is small at the beginning of the model integration (initial soil moisture depends only on land-use types in the experiment). Thus, compared to control experiment, in the desertification region evaporation decreases, cloud cover reduces, and net surface heating from solar radiation increases as a result, its surface temperature increases considerably. Transfers of long wave radiation and sensible heat flux from surface to atmosphere are intensified. Those characteristics are clearly shown by the differences between sensitivity experiment and control one (not given).

Like Fig.6, we again give differences between experiments for fluxes of surface evaporation and sensible heat to atmosphere, where evaporation or sensible heat flux is average value accumulated a day. Fig. 7 shows variations of those differences as a function of latitude. It indicates that the surface evaporation anomaly becomes negative in the middle and positive in the southern and northern parts of North China. Moreover, two positive peaks appear around 40°–50°N of the desertification region. Anomaly variation of sensible heat flux is contrary to that of surface evaporation and a larger positive anomaly appears at 40°N, that is, the central North China. There exist two peaks of negative anomaly in the desertification region and a stronger one occurs near 44°N. Variation of precipitation is closely related to those of surface evaporation and sensible heat fluxes. The curve of precipitation varies essentially in phase with that of evaporation flux while it is out of phase with that of sensible heat flux, in other words, in phase with that of downward sensible heat flux. Similarly, differences between experiments for fluxes of net solar radiation and long wave radiation from surface to atmosphere (Fig.8) also show the relationship to the precipitation variation.

Therefore, grassland desertification changes transfers of fluxes between land and atmosphere in a considerable degree. Thus, this kind of variation has no doubt an important effect on atmospheric circulation. At the center of desertification region (around 112°E in North China) we cut a cross-section of meridional circulation so that we can analyze difference of circulation between two experiments in July (Fig. 9). In the central troposphere there exist two primary secondary circulation cells. One anticlockwise circulation cell appears in the northern part of North China (the desertification region) and another clockwise circulation cell appears in the southern part. More intensive downdraft occurs in the range from 38°N to 42°N that corresponds to the positive anomaly peak of surface sensible heat flux. Around 44°–45°N there exists ascending motion of the anticlockwise circulation cell in the desertification region that corresponds to the negative anomaly valley of surface sensible heat flux. As a consequence, the variation of heat transfers between land and atmosphere can excite this kind of secondary circulation or secondary circulation cell. Its effect extends to not only the boundary layer but also almost the whole troposphere. As to the secondary circulation cell in the desertification region, for example, its ascending motion approaches $\sigma = 0.2$ level (about 300 hPa). At the same time, this kind of secondary circulation changes moisture transport in a large degree. As divergence circulation in the southern part of North China meets warm-wet air from the south, a convergence zone or center appears in the

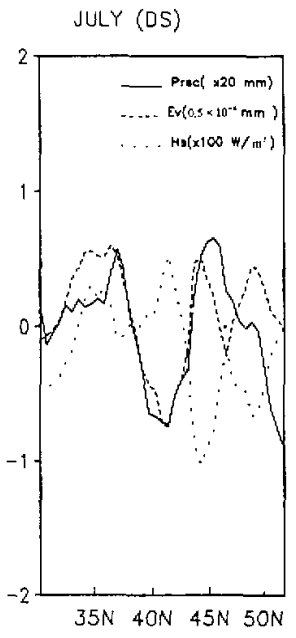

Fig. 7. Anomalies of average surface evaporation flux and sensible heat flux as a function of latitude in July. The solid line denotes rainfall, the dashed line denotes evaporation (mm / day) and the dotted line denotes sensible heat (W / m^2).

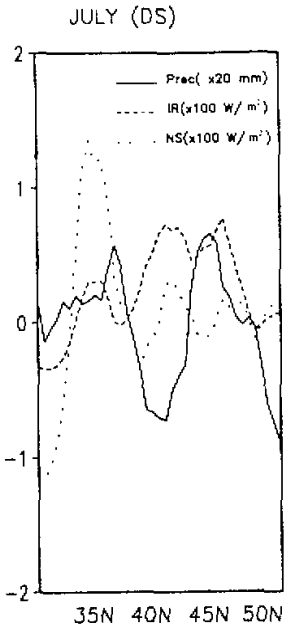

Fig. 8. Anomalies of average net surface fluxes of solar radiation and long wave radiation as a function of latitude in July. The solid line denotes rainfall, the dashed line denotes long wave radiation (W / m^2) and the dotted line denotes solar radiation (W / m^2).

Changjiang–Huaihe River Valley, while divergence circulation in the central part reduces the compensation which moisture transport makes for losses of surface evaporation here. Additionally, in the northern part of North China, the secondary circulation cell contributes to concentration of moisture near 45°N.

Variation of vertical motion can further explain the precipitation anomaly. In Fig.6 the dashed line denotes anomaly of vertical velocity ω as a function of latitude on $\sigma = 0.525$ model level (about 573 hPa level, that is, the central troposphere) and negative value of ω denotes ascending motion. Obviously, the variation of the vertical velocity agrees well with that of precipitation in July. Where ascending motion intensifies, rainfall also increases correspondingly. Similarly, where downward motion intensifies, rainfall decreases. Additionally, a similar relationship is also shown from other months except for June when two curves in the southern and central parts of North China show clearly out of phase. Considering vertical velocity in the middle and upper troposphere further, then two curves vary in phase.

If we use an arrow to denote effect of variation of a parameter on that of another one, studies mentioned above can indicate a process of the desertification effects as follows: grassland desertification (albedo, soil moisture, etc.) → evaporation → radiative and sensible heat fluxes → surface temperature → secondary circulation → moisture transport →

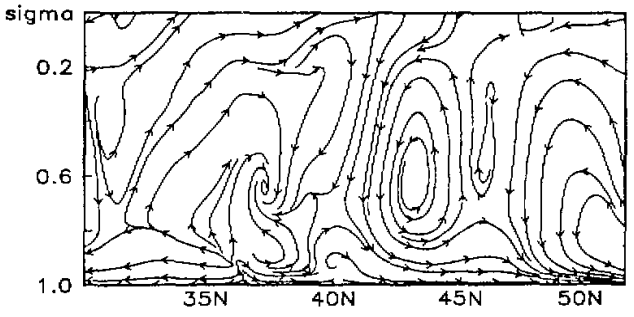

Fig. 9. Difference of meridional circulation between two experiments in July.

precipitation. It is similar to Charney's hypothesis in dynamics of deserts that the process indicates as follows: albedo→surface air temperature→large scale circulation→convergence of moisture transport→precipitation. However, evaporation is not included.

6. Conclusions

This paper has examined the effects of the grassland desertification on variation of the summer drought of 1991 in North China by using the high-resolution regional climate model RegCM2. The results are as follows:

1. The RegCM2 essentially catches the characteristics on distribution and seasonal variation of the summer precipitation in 1991 in North China, which agree well with the observation for real underlying surface. However, simulated rainfall of intensive rain bents or precitation centers shows less than observed.

2. On condition that grassland in the central and the northern parts of North China as well as in Mongolia becomes desertification, the summer accumulated precipitation decreases. In June, precipitation increases obviously in the middle and lower reaches of the Changjiang River Basin and decreases in the southern part of North China so that the intensive rainband during Mei-yu period moves southward compared to that of control experiment. Particularly during its flood period in July, precipitation in the central North China considerably decreases. Moreover, the border of rainfall or soil moisture reduction in the desertification region extends southeastward about one degree and beyond the southeast edge of desertification. Thus, vegetation in the border region approaches desertification further. There is obviously, however, different for variation of precipitation in the whole desertification region.

3. Grassland desertification changes greatly transfers of fluxes between land and atmosphere. Secondary circulation or secondary circulation cells in the desertification region and its surrounding can be excited and they change moisture transport. Variation of transfers of fluxes between land and atmosphere as well as vertical motion of atmosphere is closely related to that of precipitation.

REFERENCES

Charney J.G., 1975: Dynamics of desert and drought in the Sahel. *Quart. J. R. Met. Soc.*, **101**, 193-202.

Dickinson R.E., A. Henderson-Sellers and P.J. Kenedy, 1992: Biosphere-atmosphere transfer scheme (BATS) version 1E as coupled to the NCAR community climate model, NCAR Tech. Note NCAR / TN-387+STR, 72pp.

Girogi, F., M.R. Marinucci and G.T. Bates, 1993: Development of a second-generation regional climate model (RegCM2), Part I: boundary-layer and radiative transfer processes. *Mon. Wea. Rev.*, **121**, 2794-2813.

United Nations Food and Agriculture Organization, 1977: United Nations Map of World Desertification. *United Nations Educational Scientific and Cultural Organization and the World Meteorological Organization for the United Nations conference on Desertification*, Nairobi, Kenya.

Wang X.W., 1990: Current climate change and its evolution tendency. *The Climate Research of Drought and Flood*, China Meteorological Press, Beijing, 1-9 (in Chinese).

Xie P.P. and P. A. Arkin, 1997: Global precipitation: A 17-year monthly analysis based on Gauge observations, satellite estimates and numerical models outputs. Submitted to the Bulletin of American Meteorological Society.

Ye D.Z. and P.Q. Chen, 1992: *Preliminary study on global change in China, Part* Ⅱ, China Earthquake Press, Beijing, 279pp (in Chinese).

Ye D.Z., 1992: *Preliminary study on global change in China, Part* Ⅰ. China Meteorological Press, Beijing, 101pp (in Chinese).

Ye, J.L., S.W. Wang and X.D. Li, 1997: Study on pattern of drought and flood in East China. *Quarterly Journal of Applied Meteorology*. **8**, 69-77 (in Chinese).